The EuroBiotech Journal
RESEARCH ARTICLE
Medicine and Biotechnology

Biological effects induced by Gadolinium nanoparticles on Lymphocyte A20 cell line

Cecilia Virginia Gheran[1], Sorina Nicoleta Voicu[1,2], Guillaume Rigaux[3], Maite Callewaert[3], Francoise Chuburu[3] and Anca Dinischiotu[1]

Abstract

Gadolinium nanoparticles (GdNPs) are potential agents for MRI of lymph nodes. The aim of this study was to evaluate the *in vitro* effects of 1 μM, 2.5 μM and 5 μM of GdDOTA⊂CS-TPP/HA and GdDOTP⊂CS-TPP/HA NPs on A20 lymphocyte cells exposed for 6 and 24 hours. The total cellular biomass (SRB), lactate dehydrogenase activity (LDH) and oxidative stress parameters, such as reactive oxygen species generation (ROS), reduced glutathione (GSH), malondialdehyde (MDA) and advanced oxidation protein products (AOPP) were analyzed by spectrophotometric and fluorimetric methods. After cells exposure to 1 μM, 2.5 μM and 5 μM of GdDOTP⊂CS-TPP/HA NPs their viability decreased in a time- and dose-dependent manner, whereas for GdDOTA⊂CS-TPP/HA no significant changes were noticed. Both NPs formulations in doses of 1 μM, 2.5 μM, 5 μM did not affect the plasma membrane at each time point tested. The levels of ROS, MDA and AOPP increased proportionally with the concentration and exposure time. GSH concentration decreased significantly for all doses of both NPs tested. Taken together our data suggest that, GdDOTP⊂CS-TPP/HA and GdDOTA⊂CS-TPP/HA NPs induced oxidative stress in A20 lymphocyte cells which was counteracted by the cells antioxidant defense system to a certain extend.

[1]Department of Biochemistry and Molecular Biology, Faculty of Biology, University of Bucharest, Bucharest, Romania

[2]Department of Pharmacy, Faculty of Pharmacy, Titu Maiorescu University, Bucharest, Romania

[3]Institut de Chimie Moléculaire de Reims, CNRS UMR 7312, Université de Reims Champagne-Ardenne URCA, 51685 Reims Cedex 2, France

Corresponding author: Anca Dinischiotu
Email: anca.dinischiotu@bio.unibuc.ro

Published online: 27 January 2017
doi:10.24190/ISSN2564-615X/2017/01.09

Introduction

In the last years, the development of gadolinium-based nanoparticles (GdNPs) as contrast agents (CAs) for Magnetic Resonance Imaging (MRI) has grown exponentially, due to their interesting magnetic properties (1). Those MRI probes, that associated gadolinium chelates (GdCAs) and nano-sized objects (by covalent grafting of by encapsulation) act as catalysts to enhance the relaxation rates of tissue water proton molecules and then, to improve the image contrast in MRI. The advantage to combine GdCAs with nanoparticles is not only to enhance MRI sensitivity by improvement of image contrast (2, 3) but also to diminish the injected Gd doses. Therefore, possible side effects (4, 5) reported for some GdCAs of Nephrogenic Systemic Fibrosis (NSF) in patients with renal failure (4) can be avoided, for the benefit of the patients. Recently, confinement of GdCAs within in a hydrophilic polymeric nanostructures has allowed to pass a milestone in MRI probes efficiency (6, 7).The corresponding objects that combine an important concentration of GdCAs within high-water content nanostructure help to improve the efficacy of commercially available GdCAs by a factor of 10 to 24. These highly hydrophilic NPs also called hydrogels are obtained by ionic gelation (8-12) between two biocompatible (13) polysaccharides chitosan (CS) and hyaluronic acid (HA) in the presence of sodium tripolyphosphate (TPP) as a cross-linker (6, 7) The biocompatibility of the polymers does not presuppose that the corresponding hydrogels are biocompatible and the biocompatibility of the hydrogels incorporating the GdCA of DOTAREM, GdDOTA (DOTA = 1,4,7,10-tetraazacyclododecane-1,4,7,10-tetraacetic acid) and GdDOTP (DOTP = 1,4,7,10-tetraazacyclododecane-N,N',N",N"'-tetrakis(methylenephosphonic acid) is still poorly explored. Biodegradation, biodistribution and toxicity of chitosan were reported by T Kean et al. in a recent review (14) In this context, before considering their applica-

tions in clinical area, studies regarding nanoparticles toxicity are necessary (15).

This study aims to investigate the potential toxicity of two well-known, low risk contrast agents towards NSF i.e. GdDOTA and GdDOTP, encapsulated in a nanohydrogels constituted of CS and HA (GdDOTA⊂CS-TPP/HA and GdDOTP⊂CS-TPP/HA NPs, respectively). The *in vitro* effects of these new formulations have been evaluated on A20 murine model. The cytotoxicity and biochemical changes induced by the exposure of A20 murine lymphocyte B cells to increasing concentrations of GdDOTA⊂CS-TPP/HA and GdDOTP⊂CS-TPP/HA NPs were analyzed. For that, the total cellular biomass (SRB), lactate dehydrogenase activity (LDH) and oxidative stress parameters, such as reactive oxygen species generation (ROS), reduced glutathione (GSH), malondialdehyde (MDA) and advanced oxidation protein products (AOPP) were investigated in a time dependent manner.

Materials and Methods

Reagents

Sterile water was purchased from Laboratoire Aguettant, Lyon, France and sodium tripolyphosphate from Acros Organics. DOTA and DOTP were purchased from Macrocyclics (Dallas, USA). Chitosan (KiOmedine CsU-A), sodium hyaluronate were provided by Sigma (France) and bovine serum albumin by Sigma (New Zealand). Fetal bovine serum, RPMI-1640 medium and phosphate-buffered saline were purchased from Gibco and 2',7'-dichlorodihydrofluorescein diacetate from Invitrogen by Thermo Fisher Scientific Inc. (Waltham, MA, USA). HCl (37%), HNO_3 (69%), acetic acid glacial, potassium iodide, glucose, ethylenediaminetetraacetic acid, 5-sulfosalicylic acid, antibiotic-antimycotic solution stabilized with 10.000 units penicillin, 10 mg streptomycin and 25 µg amphotericin B per mL, *In Vitro* Toxicology Assay Kit Sulforhodamine B based, *In Vitro* Toxicology Assay Kit Lactic Dehydrogenase based, Reduced glutathione, 5,5-dithio-bis-(2-nitrobenzoic acid), thiobarbituric acid, 1,1,3,3-tetramethoxypropane and chloramine T were purchased from Sigma (St. Louis, MO, USA). Bradford reagent was provided by Bio-Rad.

Synthesis and characterization of nanoparticles

Stock solutions of CS (KiOmedine CsU-A) were prepared by dissolution of the CS powder (2.5 $mg.mL^{-1}$) in a 10% (m/v) citric acid aqueous solution and stirred overnight.

Nanoparticles were obtained by an ionotropic gelation process (6, 7). The polyanionic phase i.e. HA (0.8 $mg.mL^{-1}$) and TPP (1.2 $mg.mL^{-1}$) in water (4.5 mL), were added dropwise to the CS solution (9 mL) under sonication (750W, amplitude 32%) to obtain stable nanosuspensions. The gadolinium complex (GdDOTA or GdDOTP) was previously dissolved in the polyanion solution. At the end of the addition, magnetic stirring was maintained for 10 min. Unloaded nanoparticles were obtained in the same way, omitting the gadolinium complex. Nanosuspensions were then freeze-dried, using glucose 15% (m/v) as a cryoprotectant. NP average hydrodynamic diameters (D_H) and polydispersity indexes (PdI) were determined by Dynamic Light Scattering (DLS) (Malvern Zetasizer Nano-ZS, Malvern Instruments, Worcestershire, UK). Each nanosuspension was analyzed in triplicate at 20 °C at a scattering angle of 173°, for each sample, after 1/20 dilution in water. Pure water was used as a reference dispersing medium. ζ-(zeta) potential data were collected through electrophoretic light scattering at 20 °C, 150 V, in triplicate for each sample, after 1/20 dilution in water. The instrument was calibrated with a Malvern - 68 mV standard before each analysis cycle. Gadolinium nanoparticle loading was determined on nanoparticle suspensions by ICP-OES. The nanoparticle suspension was incubated overnight in a 1:3 (v:v) mixture of HCl (37%) and HNO_3 (69%). Volumetric dilutions were carried out to achieve an appropriate Gd concentration within the working range of the method. Samples were analysed using Thermo Scientific iCAP 6300 series Duo ICP spectrometer. Gd emission intensity was correlated to Gd concentration by means of a calibration curve which was previously established from $Gd(NO_3)_3$ ICP-OES standard. Solutions used for the calibration were obtained by dilution of increasing amounts of $Gd(NO_3)_3$ standard with unloaded nanoparticles previously incubated under acidic conditions, as described above.

Cell culture and treatment

A20 is a BALB/c B cell lymphoma line derived from a reticulum cell sarcoma found in an BALB/cAnN mouse. The cells were cultured in RPMI-1640 medium (Roswell Park Memorial Institute medium) supplemented with 1% antibiotic (penicillin, streptomycin and amphotericin B) and 10% fetal bovine serum maintained at 37°C in a humidified air atmosphere with 5% CO_2. They were seeded at a density of 2×10^5 cells/mL onto 75 cm^2 culture flasks and the experiments were carried out using cells between passages 3 and 5. The cells were exposed to 1 µM, 2.5 µM, 5 µM of GdDOTA⊂CS-TPP/HA and GdDOTP⊂CS-TPP/HA NPs for 6h and 24h. CS-TPP/HA NPs were used as controls.

Cellular lysate preparation and determination of protein concentration

A20 cells, collected from culture flasks were centrifuged at 1500 rpm for 5 min at 4°C. After removing the culture medium, the cell pellet was washed with phosphate-buffered saline (PBS) two times and centrifuged again in the same conditions. Cell pellets were resuspended in 0.3 mL of PBS and then, homogenized by sonication using Hielscher Ultrasonic processor UP50H on ice three times, for 30 seconds each. The cellular lysate was centrifuged at 5000 rpm for 10 min at 4°C. The supernatant was decanted, aliquoted and stored at -80°C and used for further biochemical determinations. The total protein concentration was measured according to the method described by Bradford (16) using bovine serum albumin (BSA) as a standard. The absorbance was spectrophotometrically measured at a wavelength of 595 nm using the Appliskan Thermo Scientific Multireader and the results were expressed as $mg.mL^{-1}$.

Sulforhodamine assay (SRB)

The viability of A20 cells was assessed using the *in vitro* Toxicology Assay Kit, Sulforhodamine B based (Sigma-Aldrich, St. Louis, MO, USA) and following manufacturer's instructions. This method is based on the measurement of total biomass by staining cellular proteins with the Sulforhodamine B dye. After 6 and 24h of exposure to 1 µM, 2.5 µM, 5µM Gd-DOTA⊂CS-TPP/HA and GdDOTP⊂CS-TPP/HA NPs, cells were fixed with 50% trichloroacetic acid (TCA) solution (1/4 volume of growth medium) for 1 hour at 4°C. Then, cells were washed with distilled water several times and the plates were air dried. Cells were then stained for 20 minutes at room temperature in the presence of a 0.4% sulforhodamine B (Acid Red 52) solution. The dye was then removed and the cells washed with a solution of acetic acid 1% (v:v). In order to solubilize the sulforhodamine B dye incorporated into the cells a 10mM Tris base solution was used. The absorbance was spectrophotometrically measured at a wavelength of 550 nm using the Appliskan Thermo Scientific Multireader.

Lactate dehydrogenase release (LDH)

Lactate dehydrogenase (LDH) activity was evaluated using a commercial kit, *in vitro* Toxicology Assay Kit, Lactic Dehydrogenase based (Sigma-Aldrich, St. Louis, MO, USA) according to the manufacturer's instructions. The cell membrane integrity was estimated as a function of the quantity of LDH released into the cell culture medium. The method is based on the reduction of nicotinamide adenine dinucleotide (NAD^+) in the presence of lactate and LDH, followed by the conversion of a tetrazolium dye into a colored formazan compound which can be spectrophotometrically quantified at 450 nm. A total of 2×10^5 A20 cells per mL were seeded in 24-well cell culture plates. After 24h of incubation, the cells were exposed to concentrations of 1 µM, 2.5 µM, 5 µM of GdDOTA⊂CS-TPP/HA and GdDOTP⊂CS-TPP/HA NPs for 6 and 24 h. A volume of 50 µL of each sample was placed on a 96-well microtiter plate and then 100 µL of lactate dehydrogenase assay mixture were added. After 30 min at room temperature, the reaction was stopped by adding 1/10 volume of HCl 1M M to each well and the absorbance was read spectrophotometrically at a wavelength of 450 nm using the Tecan GENios Multireader. The LDH activity was expressed as % of controls (cells treated with unloaded CS-TPP/HA NPs).

Lipid peroxidation measurement (MDA)

The level of malondialdehyde (MDA), a marker for oxidative degradation of lipids was assessed using thiobarbituric acid (TBA) as a reagent according to Dinischiotu et al. (17). A volume of 200 µL of cell lysate with a total protein concentration of 3 mg. mL^{-1} was mixed with 700 µL of HCl 0.1 M and incubated at room temperature for 20 min. Afterwards, 900 µL of 0.025 M thiobarbituric acid were added and the mixture was maintained for 65 min at 37°C. Finally, 400 µL of PBS were added. The fluorescence of MDA-TBA adduct was quantified fluorometrically ($\lambda_{exc/em}$ =520/549 nm) using a Jasco FP-750 spectrofluorometer (Tokyo, Japan). MDA concentration was calculated using a 1,1,3,3-tetramethoxy propane calibration curve with concentrations in the range of 0.5-5 µM. The results were expressed as nmoles of MDA per mg of protein.

Reduced glutathione assay (GSH)

The GSH concentration was determined using the Glutathione Assay Kit (Sigma-Aldrich, St. Louis, MO, USA) following manufacturer's instructions. Briefly, cellular lysates were deproteinized with an equal volume of 5% 5-sulfosalicylic acid (SSA) and centrifuged at 10000 rpm for 10 minutes at 4°C. A volume of 10 µL of each supernatant was placed on a 96-well microtiter plate. Then 150 µL of working mixture containing 8 mL of 100 mM potassium phosphate buffer, pH 7.0, with 1 mM ethylenediaminetetraacetic acid (EDTA) - assay Buffer and 228 µL of 1.5 $mg.mL^{-1}$ 5,5'-dithiobis-(2-nitro benzoic acid) (DTNB) were added. After 5 minutes of incubation at room temperature, the absorbance of 5-thio-2-nitrobenzoic acid (TNB) was measured spectrophotometrically at a wavelength of 412 nm using the Tecan GENios Multireader. In order to determine the amount of glutathione in the samples, a calibration curve of GSH in the range of 0.5-0.03 nmoles was used. The results were expressed as nmoles of GSH per mg of protein.

Determination of intracellular reactive oxigen species (ROS)

Detection of intracellular ROS in A20 cells was assessed using a chemically reduced, acetylated form of fluorescein, 2',7'-dichlorodihydrofluorescein diacetate (H_2DCFDA) (18). This nonfluorescent compound is converted to a green-fluorescent form upon cleavage of the acetate groups by cellular esterases and oxidation occurs within the cell. A20 cells were seeded in six-well plates at a density of 2×10^5 cells mL^{-1}.

After exposure to 1 µM and 5 µM of GdDOTA⊂CS-TPP/HA and GdDOTP⊂CS-TPP/HA NPs for 6h and 24h, the cells were incubated with 10 µM of H_2DCFDA in the dark for 30 minutes at 37°C. Then, cells were collected by centrifugation at 250 *g* for 4 minutes, the pellets were washed twice and resuspended in 2 mL of PBS solution. The fluorescence of dichlorofluorescein (DCF) was quantified fluorometrically ($\lambda_{exc/em}$ = 488/515 nm) using a Jasco FP-750 spectrofluorometer (Tokyo, Japan). The results were calculated by dividing the fluorescence intensity to the number of viable cells and expressed as % of controls (cells treated with unloaded CS-TPP/HA NPs).

Advanced oxidation protein products assay (AOPP)

The level of AOPP, a marker of oxidative stress was analyzed using the method described by Witko-Sarsat et al. (19). 200 µL of cell lysate was mixed with 10 µL of 1.16 M potassium iodide and vortexed for 5 minutes at room temperature. A volume of 20 µL of glacial acetic acid was added and then the mixture was vortexed again for 30 seconds. The sample's optical density was read at a wavelength of 340 nm using a Tecan GENios Multireader. Spectrophotometric determination of AOPP was calculated based on a chloramine T calibration curve with con-

centrations up to 100 μM. The results were expressed as nmoles of AOPP per mg of protein.

Statistical analysis

The results were expressed as mean value of triplicate experiments ± standard deviation (SD) and compared by Student's *t*-test using standard statistical packages. Data were represented as graphics relative to control which was considered 100%. Statistical significance was accepted for a *p* value less than 0.05.

Results

Sulforhodamine B assay (SRB)

A20 murine B lymphocytes viability in the presence of different concentrations (1, 2.5 and 5 μM) of GdDOTA⊂CS-TPP/HA and GdDOTP⊂CS-TPP/HA NPs for 6 and 24h was presented in **Fig. 1**.

When A20 cells were treated with GdDOTA⊂CS-TPP/HA NPs, no significant NPs impact was encountered on cell viability at any doses tested up to 24h. In the case of cell exposure to GdDOTP⊂CS-TPP/HA NPs, a time- and dose-dependent decrease of cell viability was observed. Thus, after 24h, the cell viability decreased by 18% at the lowest concentrations and 28% at the highest.

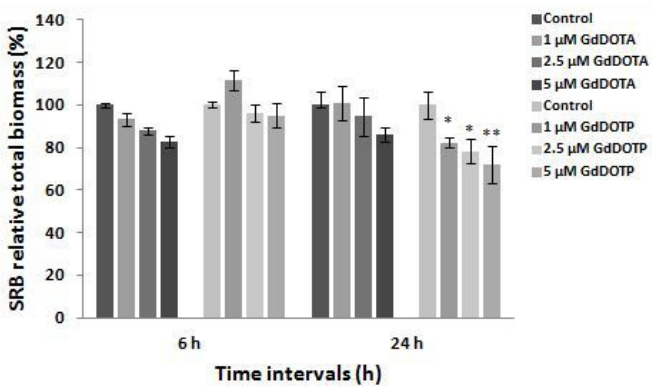

Figure 1. Viability cell (SRB assay) of A 20 cells after exposure to 1 μM, 2.5 μM, 5 μM GdDOTA⊂CS-TPP/HA and GdDOTP⊂CS-TPP/HA NPs for 6h and 24 h. Unloaded CS-TPP/HA NPs were used as control. Results are calculated as means ± SD (n = 3) and expressed as % from controls. *$p < 0.05$; ** $p < 0.01$

LDH release

The cytotoxic potential of Gd⊂CS-TPP/HA NPs on A20 cells was evaluated by testing the cell membrane integrity via LDH leakage in the culture medium.

Fig. 2 showed that both nanoparticle formulations in doses of 1 μM, 2.5 μM, 5 μM did not affect the plasma membrane at each time points, since no significant amount of LDH was released to cell culture medium, as compared to control (CS-TPP/HA NPs).

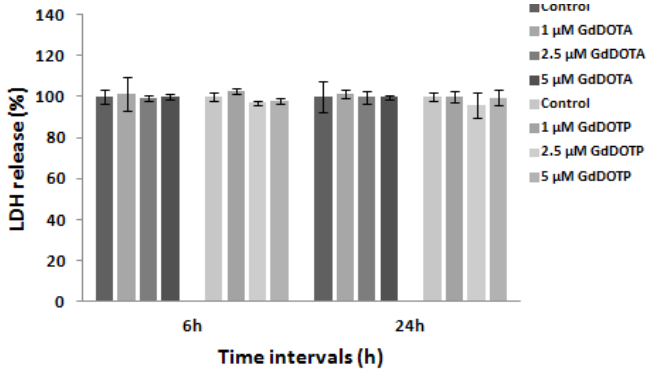

Figure 2. LDH release from A 20 cells after exposure to 1 μM, 2.5 μM, 5 μM GdDOTA⊂CS-TPP/HA and GdDOTP⊂CS-TPP/HA NPs for 6h and 24 h. Unloaded CS-TPP/HA NPs were used as control. Results are calculated as means ± SD (n = 3) and expressed as % from controls.

Determination of intracellular ROS

ROS level proved that exposure of A20 cells to both types of nanoparticles generated a rise of ROS production in a time dependent manner for the higher concentration (**Fig. 3**).

A significant increase in ROS levels by 16% and 25% was noticed in A20 cells exposed to 5 μM GdDOTP⊂CS-TPP/HA after 6h and 24h, respectively, as compared to control (CS-TPP/HA NPs) whereas for GdDOTA⊂CS-TPP/HA treatment the increase was insignificant.

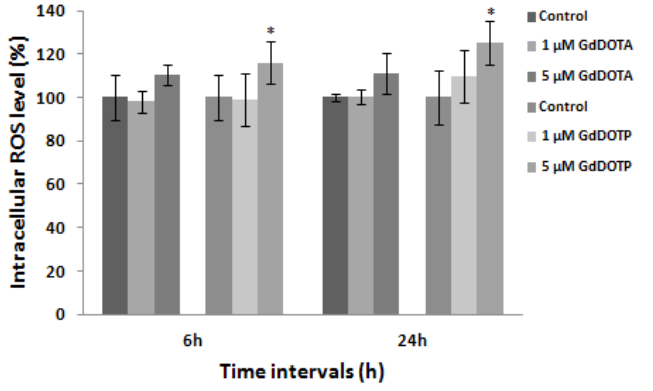

Figure 3. Reactive oxygen species (ROS) production in A20 cells, after exposure to 1 μM and 5 μM NPs GdDOTA⊂CS-TPP/HA and GdDOTP⊂CS-TPP/HA for 6h and 24 h. Unloaded CS-TPP/HA NPs were used as control. Results are calculated as means ± SD (n = 3) and expressed as % from controls.

Lipid peroxidation (MDA), reduced glutathione (GSH) and advanced oxidation protein products (AOPP) in A20 cells

A time- and dose-dependent increase in the MDA level in A20 cells was registered compared to control (**Table 1**).

Significant MDA level increases of 15% and 17% were observed after 6h of exposure to 5 μM GdDOTA⊂CS-TPP/HA and GdDOTP⊂CS-TPP/HA respectively, and by 16% and 21% after 24h.

The concentrations of GSH, a non-enzymatic antioxidant decreased in a significant statistically manner, compared to

Table 1. Relative values of lipid peroxidation (MDA), reduced glutathione (GSH) and advanced oxidation protein products (AOPP) in A20 cells, after exposure to 1 μM and 5 μM GdDOTA⊂CS-TPP/HA and GdDOTP⊂CS-TPP/HA NPs for 6h and 24 h. Unloaded CS-TPP/HA NPs were used as control.

Time (h)	Nanoparticles	MDA (nmoles/mg) Control	1 μM	5 μM	GSH (nmoles/mg) Control	1 μM	5 μM	AOPP (nmoles/mg) Control	1 μM	5 μM
6 h	GdDOTA	100±8	102±2	115±8 *	100±4	96±8	93±7	100±5	101±5	106±2
	GdDOTP	100±10	102±4	117±6 *	100±5	95±4	90±3 *	100±6	102±9	119±4 **
24 h	GdDOTA	100±5	110±5	116±10 *	100±9	95±8	89±7 *	100±9	108±3	111±11
	GdDOTP	100±6	113±9	121±3 **	100±6	89±2	82±6 **	100±7	109±9	148±12 **

Note: Results are calculated as means ± SD (n = 3) and expressed as % from controls; *$p < 0.05$; ** $p < 0.01$

controls (**Table 1**). Thus, GSH levels were reduced after 6h of exposure for both NP doses tested. The decrease was amplified till 5% and 11% after 24h for 1 μM and 11% and 18% for 5 μM GdDOTA⊂CS-TPP/HA and GdDOTP⊂CS-TPP/HA, respectively.

Finally, AOPP concentrations were not significantly changed at any GdDOTA⊂CS-TPP/HA doses tested up to 24h of exposure, whereas significant increases up to 19% and 48% were recorded after 6h and 24h of cell exposure to the higher concentration of GdDOTP⊂CS-TPP/HA NPs, compared to control.

Discussion

Despite the gaining popularity of Gd(III) contrast agents in the medical field, their potential toxicity and long-term adverse side effects represent an important concern (20-24). In order to improve these aspects, new nanocarriers which are characterized by a good biodegradability, water-solubility, controlled drug release and low toxicity are now receiving a growing interest for Gd-based contrast agents vectorization (25-29).

Being designed for *in vivo* applications, especially for lymph node imaging, the evaluation of the potential toxicity generated by GdDOTA and GdDOTP nanocarriers (GdDOTA⊂CS-TPP/HA and GdDOTP⊂CS-TPP/HA) is essential for their future applications.

The first step towards understanding the way in which nanoparticles interact with cells often involves *in vitro* cell culture studies. Murine models of B-cell lymphomas are considered to be promising tools for development of cancer studies (30, 31) and can determine a massive invasion of liver, spleen and lymph nodes (32, 33) Previously it was demonstrated that some nanoparticles induce oxidative stress on lymphocytes and lymph nodes which could lead to their damage (34). For these reasons A20 cell line was selected as a model for *in vitro* experiments.

Several studies have revealed that Gd-based contrast agents induced apoptosis and necrosis in different cell types (renal tubular cells, human foreskin fibroblasts (HFFs), NIH/3T3 fibroblasts) in a time (35) -and dose (36, 37) -dependent manner. By contrast, another research group has demonstrated the safety of a new designed multifunctional MRI contrast agents against HepG2 cells at the test concentrations, after 24h of incubation (38) Lack of toxic effects induced by different doses of gadolinium loaded chitosan and chitosan-hyaluronic acid nanoparticles in three cell lines (B16, HepG2, and A549 cells) at the same time point, were also reported (39, 40). Likewise, hydrogels incorporating GdDOTA and GdDOTP did not exhibit any toxicity towards C6 glioma or primary fibroblasts cells (6, 7).

Sulforhodamine B viability tests suggested that GdDOTP⊂CS-TPP/HA NPs were more toxic for A-20 cells compared to GdDOTA⊂CS-TPP/HA ones. These results were not confirmed by LDH activity in the culture medium probably due to a lesser sensitivity of the enzymatic method.

Feng X. et al. have reported a remarkable increase in LDH leakage, after exposure of rat cortical neuron cells to $GdCl_3$ (0.2, 2, 20 and 100 μM) even at low micromolar doses (41). Almost in the same time, Xia Q. et al. (42) revealed that $GdCl_3$ (0.2, 2, and 20 μM) induced in neurons a decrease of cell viability and an increase of LDH released onto the culture medium in a time- and concentration-dependent manner (43). Our data are not in accordance with these two studies, due to the fact that in our experiments Gd^{3+} was firstly complexed by DOTA or DOTP and secondly embedded in the nanogels.

The mechanisms by which Gd-based nanoparticles enters the cells are not entirely understood. Some studies demonstrated that, these nanoparticles are generally transported to cells by endocytic pathway depending on their size, shape and nature (44). Thus, mechanisms such as macropinocytosis (45), clathrin-mediated endocytosis (46), receptor-mediated endocytosis (47) were proposed. Dodane and Vilivalam reported that, chitosan and chitosan nanoparticles due to their positive charge,

enter the cells via cell membrane depolarization, leading to an increased Ca^{2+} influx (48).

Gd-based contrast agents have been intensively investigated with main focus on nephrotoxicity and nephrogenic systemic fibrosis (NSF) in patients with severe renal impairment (49-53). Our experiment showed that, both types of nanoparticles at a concentration of 5 μM induced moderate levels of reactive oxygen species in A-20 cells.

Lipid peroxidation is a process generated by the action of reactive oxygen species on polyunsaturated fatty acids. Malondialdehyde (MDA) the end product of lipid peroxidation is considered a mutagenic secondary product (54). In the present work, significant increases of MDA level, by 16% and 21% after 24h of exposure to 5 μM GdDOTA⊂CS-TPP/HA and GdDOTP⊂CS-TPP/HA, respectively show that, the antioxidant system of A20 cells counteracted an extensive damage of lipids. After exposure of human bladder tumor cells 5637 to chitosan, it was suggested that chitosan could induce apoptosis via caspase-3 activation, without the generation of MDA (55). This suggests that the peroxidation cascade occurs differently in a cell type dependent manner.

GSH is the principal non-protein thiol in cells and a ROS scavenger molecule, being involved in maintaining intra- and extracellular redox environments (56, 57). GSH depletion, as a consequence of the oxidative stress was observed in peripheral blood mononuclear cells (PBMC) exposed to low-dose Gd-Tex (58).

In our experiment, the decrease of GSH level registered in cells exposed to GdDOTA⊂CS-TPP/HA and GdDOTP⊂CS-TPP/HA- was correlated with the increase of MDA concentration.

The disturbance of the natural balance between pro-oxidant species and antioxidant systems in favor of the former, causes proteins oxidation. AOPP are formed via myeloperoxidase-H_2O_2-halide system (59) and their role in activation of human neutrophil and monocyte oxidative metabolism was previously shown (60).

In our work, significant increases of AOPP, by 19% and 48%, were recorded after exposure to the higher concentration of GdDOTP⊂CS-TPP/HA NPs for 6h and 24h, respectively related to control, which are in a close correlation with GSH and MDA results.

Conclusions

Our data suggest that GdDOTP⊂CS-TPP/HA NPs and GdDOTA⊂CS-TPP/HA NPs induced a moderate oxidative stress in A 20 cells which resulted in a slight decrease of GSH level and increase of MDA and AOPP concentrations. These effects were more pronounced in the case of GdDOTP⊂CS-TPP/HA NPs exposure. According to these, it appears that the cells antioxidant defense system counteracted to a certain extend the induced oxidative stress. Taking into account all of these, it appears that these NPs could be used in injectable formulations for MRI diagnostic.

Acknowledgements

This work was supported by Romanian National Authority for Scientific Research CCCDI-UEFISCDI (project number 4-006/2014, EuroNanoMed II) and ANR (Gadolymph project n°ANR-13-ENM2-0001-01, through the EuroNanoMed 2013 framework).

Conflict of interest statement

The authors declare no conflict of interest.

References

1. Delli Castelli D, Gianolio E, Geninatti Crich S, Terreno E, Aime S. Metal containing nanosized systems for MR-Molecular Imaging applications. Coordin Chem Rev 2008; 252(21-22): 2424–2443.
2. Merbach AS, Helm L, Toth E. The Chemistry of Contrast Agents in Medical Magnetic Resonance Imaging, 2013, Wiley and Sons, Chichester, 2nd Edn.
3. Geraldes CFGC, Laurent S. Classification and basic properties of contrast agents for magnetic resonance imaging. Contrast Media Mol I 2009; 4(1): 1–23.
4. Idée JM, Port M, Medina C, Lancelot E, Fayoux E, Ballet S, Corot C. Possible involvement of gadolinium chelates in the pathophysiology of nephrogenic systemic fibrosis: a critical review. Toxicology 2008; 248(2-3): 77–88.
5. Rogosnitzky M, Branch S. Gadolinium-based contrast agent toxicity: a rewiew of known and proposed mechanisms. Biometals 2016; 29: 365-376.
6. Courant T, Roullin VG, Cadiou C, Callewaert M, Andry MC, Portefaix C, Hoeffel C, de Goltstein MC, Port M, Laurent S, Vander Elst L, Muller R, Molinari M, Chuburu F. Hydrogels incorporating GdDOTA: towards highly efficient dual T_1/T_2 MRI contrast agents Angew Chem Int Edit 2012; 51: 9119-9122.
7. Callewaert M, Roullin VG, Cadiou C, Millart E, Van Gulik L, Andry MC, Portefaix C, Hoeffel C, Laurent S, Vander Elst L, Muller R, Molinari M, Chuburu F. Tuning the composition of biocompatible Gd nanohydrogels to achieve hypersensitive dual T1/T2 MRI contrast agents. J Mater Chem B 2014; 2: 6397–6405.
8. Fang JY, Chen JP, Leu YL, Hu JW. Temperature-sensitive hydrogels composed of chitosan and hyaluronic acid as injectable carriers for drug delivery. Eur J Pharm Biopharm 2008; 68(3): 626–636.
9. Oyarzun-Ampuero FA, Brea J, Loza MI, Torres D, Alonso MJ. Chitosan–hyaluronic acid nanoparticles loaded with heparin for the treatment of asthma. Int J Pharm 2009; 381(2): 122–129.
10. Luo Y, Wang Q. Recent development of chitosan-based polyelectrolyte complexes with natural polysaccharides for drug delivery. Int J Biol Macromol 2014; 64: 353-367.
11. Al-Qadi S, Alatorre-Meda M, Zaghloul EM, Taboada P, Remunán-López C. Chitosan-hyaluronic acid nanoparticles for gene silencing: The role of hyaluronic acid on the nanoparticles' formation and activity. Colloid Surface B 2013; 103: 615–623.
12. Deng X, Cao M, Zhang J, Hu K, Yin Z, Zhou Z, Xiao X, Yang Y, Sheng W, Wu Y. Hyaluronic acid-chitosan nanoparticles for co-delivery of MIR-34A and doxorubicin in therapy against triple negative breast cancer. Biomaterials 2014; 35(14): 4333–4344.
13. Liu Z, Jiao Y, Wang Y, Zhou C, Zhang Z. Polysaccharides-based nanoparticles as drug delivery systems. Adv Drug Deliver Rev

2008; 60(15): 1650–1662.
14. Kean T, Thanou M. Biodegradation, biodistribution and toxicity of chitosan. Adv Drug Deliver Rev 2010; 62(1): 3–11.
15. Lewinski N, Colvin V, Drezek R. Cytotoxicity of nanoparticles. Small 2008; 4(1): 26–49.
16. Bradford MM. A rapid and sensitive method for the quantitation of microgram quantities of protein utilizing the principle of protein-dye binding Anal Biochem 1976; 72: 248–254.
17. Dinischiotu A, Stanca L, Gradinaru D, Petrache SN, Radu M, Serban A. Chapter 10, Lipid Peroxidation due to in vitro and in vivo exposure of biological samples to nanoparticles. In Oxidative Stress and Nanotechnology: Methods and Protocols, Methods in Molecular Biology 2013, Armstrong D, Bharali, DJ, Eds., Springer Science Business Media: New York, NY, USA, 1028: 155–164.
18. Wan CP, Myung E, Lau BH. An automated microfluorometric assay for monitoring oxidative burst activity of phagocytes. J Immunol Methods 1993; 159(1-2): 131–138.
19. Witko-Sarsat V, Nguyen AT, Descamps-Latscha B. Microtiter plate assay for phagocyte-derived taurine-chloramines. J Clin Lab Anal 1992; 6(1): 47-53.
20. Greenberg SA. Zinc transmetallation and gadolinium retention after MR imaging: case report. Radiology 2010; 257(3): 670–673.
21. Marckmann P, Skov L, Rossen K, Dupont A, Damholt MB, Heaf JG, Thomsen HS. Nephrogenic systemic fibrosis: suspected causative role of gadodiamide used for contrast-enhanced magnetic resonance Imaging. J Am Soc Nephrol 2006; 17: 2359–2362.
22. Aime S, Caravan P. Biodistribution of gadolinium-based contrast agents, including gadolinium deposition. J Magn Reson Imaging 2009; 30(6): 1259–1267.
23. Xia D, Davis RL, Crawford JA, Abraham JL. Gadolinium released from MR contrast agents is deposited in brain tumors: in situ demonstration using scanning electron microscopy with energy dispersive X-ray spectroscopy. Acta Radiol 2010; 51(10): 1126–1136.
24. Darrah TH, Prutsman-Pfeiffer JJ, Poreda RJ, Ellen Campbell M, Hauschka PV, Hannigan RE. Incorporation of excess gadolinium into human bone from medical contrast agents. Metallomics 2009; 1(6): 479–488.
25. Agnihotri SA, Mallikarjuna NN, Aminabhavi TM. Recent advances on chitosan-based micro- and nanoparticles in drug delivery. J Control Release 2004; 100(1): 5–28.
26. Yan GP, Xu W, Yang L, Li L, Liu F, Guo QZ. Dextran gadolinium complexes as contrast agents for magnetic resonance imaging to sentinel lymph nodes. Pharm Res 2010; 27(9): 1884-1892.
27. Darras V, Nelea M, Winnik FM, Buschmann MD. Chitosan modified with gadolinium diethylenetriaminepentaacetic acid for magnetic resonance imaging of DNA/chitosan nanoparticles. Carbohyd Polym 2010; 80(4): 1137-1146.
28. Chen Z, Yu D, Liu C, Yang X, Zhang N, Ma C, Song J, Lu Z. Gadolinium-conjugated PLA-PEG nanoparticles as liver targeted molecular MRI contrast agent. J Drug Target 2011; 19(8): 657-665.
29. Ge Y, Zhang Y, He S, Nie F, Teng G, Gu N. Fluorescence modified chitosan coated magnetic nanoparticles for high-efficient cellular imaging. Nanoscale Res Lett 2009; 4: 287-295.
30. Donnou S, Galand C, Touitou V, Sautès-Fridman C, Fabry Z, Fisson S. Murine Models of B-Cell Lymphomas: Promising Tools for Designing Cancer Therapies. Adv Hematol 2012; 1-13.
31. Palmieri C, Falcone C, Iaccino E, Tuccillo FM, Gaspari M, Trimboli F, De Laurentiis A, Luberto L, Pontoriero M, Pisano A, Vecchio E, Fierro O, Panico MR, Larobina M, Gargiulo S, Costa N, Dal Piaz F, Schiavone M, Arra C, Giudice A, Palma G, Barbieri A, Quinto I, Scala G. In vivo targeting and growth inhibition of the A20 murine B-cell lymphoma by an idiotype-specific peptide binder. Blood 2010; 116(2): 226-238.
32. Chaise C, Itti E, Petegnief Y, Wirquin E, Copie-Bergman C, Farcet JP, Delfau-Larue MH, Meignan M, Talbot JN, Molinier-Frenkel V. (F-18)-Fluoro-2-deoxy-D-glucose positron emission tomography as a tool for early detection of immunotherapy response in a murine B cell lymphoma model. Cancer Immunol Immun 2007; 56: 1163–1171.
33. Siegel S, Wagner A, Schmitz N, Zeis M. Induction of antitumour immunity using survivin peptide-pulsed dendritic cells in a murine lymphoma model. Brit J Haematol 2003; 122: 911–914.
34. Buzea C, Pacheco Blandino II, Robbie K. Nanomaterials and nanoparticles:Sources and toxicity. Biointerphases 2007; 2(4): MR17 - MR172.
35. Avti PK, Caparelli ED, Sitharaman B. Cytotoxicity, cytocompatibility, cell-labeling efficiency, and in vitro cellular magnetic resonance imaging of gadolinium-catalyzed single-walled carbon nanotubes. J Biomed Mater Res A 2013; 101A(12): 3580-3591.
36. Heinrich MC, Kuhlmann MK, Kohlbacher S, Scheer M, Grgic A, Heckmann MB, Uder M. Cytotoxicity of Iodinated and Gadolinium-based Contrast Agents in Renal Tubular Cells at Angiographic Concentrations:In Vitro Study. Radiology 2007; 242(2): 425-434.
37. Do C, Barnes JL, Tan C, Wagner B. Type of MRI contrast, tissue gadolinium, and fibrosis. Am J Physiol-Renal 2014; 307: F844–F855.
38. Liu Y, Chen Z, Liu C, Yu D, Lu Z, Zhang N. Gadolinium-loaded polymeric nanoparticles modified with Anti-VEGF as multifunctional MRI contrast agents for the diagnosis of liver cancer. Biomaterials 2011; 32(22): 5167-5176.
39. Zhang L, Liu Y, Yu D, Zhang N. Gadolinium-Loaded Chitosan Nanoparticles as Magnetic Resonance Imaging Contrast Agents for the Diagnosis of Tumor. J Biomed Nanotechnol 2013; 9: 863–869.
40. Zhang L, Liu T, Xiao Y, Yu D, Zhang N. Hyaluronic Acid-Chitosan Nanoparticles to Deliver Gd-DTPA for MR Cancer Imaging. Nanomaterials 2015; 5(3): 1379-1396.
41. Feng X, Xia Q, Yuan L, Yang X, Wang K. Impaired mitochondrial function and oxidative stress in rat cortical neurons: Implications for gadolinium-induced neurotoxicity. Neurotoxicology 2010; 31: 391–398.
42. Xia Q, Feng XD, Yuan L, Wang K, Yang XD. Brain-derived neurotrophic factor protects neurons from $GdCl_3$-induced impairment in neuron-astrocyte co-cultures. Sci China Chem 2010; 53(10): 2193–2199.
43. Xia Q, Feng X, Huang H, Du L, Yang X, Wang K. Gadolinium-induced oxidative stress triggers endoplasmic reticulum stress in rat cortical neurons. J Neurochem 2011; 117(1): 38–47.
44. Kumari A, Yadav SK. Cellular interactions of therapeutically delivered nanoparticles. Expert Opin Drug Del 2011; 8(2): 141-151.
45. Rima W, Sancey L, Aloy MT, Armandy E, Alcantara GB, Epicier T, Malchère A, Joly-Pottuz L, Mowat P, Lux F, Tillement O, Burdin

B, Rivoire A, Boulé C, Anselme-Bertrand I, Pourchez J, Cottier M, Roux S, Rodriguez-Lafrasse C, Perriat P. Internalization pathways into cancer cells of gadolinium-based radiosensitizing nanoparticles. Biomaterials 2013; 34: 181-195.
46. Štefančíková L, Porcel E, Eustache P, Li S, Salado D, Marco S, Guerquin-Kern JL, Réfrégiers M, Tillement O, Lux F, Lacombe S. Cell localisation of gadolinium-based nanoparticles and related radiosensitising efficacy in glioblastoma cells. Cancer Nanotechnology 2014; 5(6): 1-15.
47. Oyewumi MO, Yokel RA, Jay M, Coakley T, Mumper RJ. Comparison of cell uptake, biodistribution and tumor retention of folate-coated and PEG-coated gadolinium nanoparticles in tumor-bearing mice. J Control Release 2004; 95: 613– 626.
48. Dodane V, Vilivalam VD. Pharmaceutical applications of chitosan. Pharm Sci Technol To 1998; 1: 246–253.
49. Bose C, Megyesi JK, Shah SV, Hiatt KM, Hall KA, Karaduta O, Swaminathan S. Evidence suggesting a role of iron in a mouse model of nephrogenic systemic fibrosis. PLoS ONE 2015; 10(8): e0136563.
50. Chen R, Ling D, Zhao L, Wang S, Liu Y, Bai R, Baik S, Zhao Y, Chen C, Hyeon T. Parallel comparative studies on mouse toxicity of oxide nanoparticle- and gadolinium-based T1 MRI contrast agents. ACS Nano 2015; 9(12): 12425–12435.
51. Idée JM, Fretellier N, Robic C, Corot C. The role of gadolinium chelates in the mechanism of nephrogenic systemic fibrosis: A critical update. Crit Rev Toxicol 2014; 44: 895–913.
52. Pereira LVB, Shimizu MHM, Rodrigues LPMR, Leite CC, Andrade L, Seguro AC. N-acetylcysteine protects rats with chronic renal failure from gadolinium-chelate nephrotoxicity. PLoS ONE 2012; 7(7): e39528.
53. Ramalho J, Semelka RC, Ramalho M, Nunes RH, AlObaidy M, Castillo M. Gadolinium-based contrast agent accumulation and toxicity: an update. Am J Neuroradiol 2015; 1-7.
54. Repetto M, Semprine J, Boveris A. Lipid Peroxidation: Chemical Mechanism, Biological Implications and Analytical Determination. InTech 2012, Chapter 1, 3-31.
55. Hasegawa M, Yagi K, Iwakawa S, Hirai M. Chitosan Induces Apoptosis via Caspase-3 Activation in Bladder Tumor Cells. Jpn J Cancer Res 2001; 92: 459–466.
56. Sies H. Glutathione and its role in cellular functions. Free Radical Bio Med 1999; 27(9/10): 916–921.
57. Pastore A, Federici G, Bertini E, Piemonte F. Analysis of glutathione: implication in redox and detoxification. Clin Chim Acta 2003; 333(1): 19–39.
58. Perez OD, Nolan GP, Magda D, Miller RA, Herzenberg LA. Motexafin gadolinium (Gd-Tex) selectively induces apoptosis in HIV-1 infected CD4+ T helper cells. Proc Natl Acad Sci U S A 2002; 99(4): 2270–2274.
59. Capeillere-Blandin C, Gausson V, Descamps-Latscha B, Witko-Sarsat V. Biochemical and spectrophotometric significance of advanced oxidized protein products. Biochim Biophys Acta 2004; 1689: 91-102.
60. Witko-Sarsat V, Gausson V, Nguyen AT, Touam M, Drüeke T, Santangelo F, Descamps-Latscha B. AOPP-induced activation of human neutrophil and monocyte oxidative metabolism: A potential target for N-acetylcysteine treatment in dialysis patients. Kidney Int 2003; 64: 82–91.